A strain affiliated to Bacillus amyloliquefaciens alleviates high-carbohydrate diet- induced metabolic syndrome by restoration of acetate-producing bacteria in fish intestines

Rong Xu
East China Normal University
Miao Li
East China Normal University
Tong Wang
East China Normal University
Yi-Wei Zhao
East China Normal University
Cheng-Jie Shan
East China Normal University
Fang Qiao
East China Normal University
Li-Qiao Chen
East China Normal University
Zhen-Yu Du
East China Normal University
Mei-Ling Zhang (mlzhang@bio.ecnu.edu.cn)
East China Normal University https://orcid.org/0000-0003-2689-8720

Research

Keywords: Nile tilapia, Intestinal microbiota, SCFA, Metabolism, GLP-1, Carbohydrate utilization

Posted Date: May 14th, 2020

DOI: https://doi.org/10.21203/rs.3.rs-27653/v1

A strain affiliated to *Bacillus amyloliquefaciens* alleviates high-carbohydrate diet-induced metabolic syndrome by restoration of acetate-producing bacteria in fish intestines

Rong Xu, Miao Li, Tong Wang, Yi-Wei Zhao, Cheng-Jie Shan, Fang Qiao, Li-Qiao Chen, Zhen-Yu Du* and Mei-Ling Zhang*

LANEH, School of Life Sciences, East China Normal University, Shanghai 200241, China

* Correspondence: mlzhang@bio.ecnu.edu.cn; zydu@bio.ecnu.edu.cn

Author details

Rong Xu: 52181300029@stu.ecnu.edu.cn;

Miao Li: 784662878@qq.com;

Tong Wang: 1433918962@qq.com;

Yi-Wei Zhao: 1764548528@qq.com;

Cheng-Jie Shan: 1515509277@qq.com;

Fang Qiao: fqiao@bio.ecnu.edu.cn;

Li-Qiao Chen: lqchen@bio.ecnu.edu.cn;

Zhen-Yu Du: zydu@bio.ecnu.edu.cn;

Mei-Ling Zhang: mlzhang@bio.ecnu.edu.cn.

Abstract

Background: Increasing the utilization efficiency of high-carbohydrate diet has the potential to promote "protein sparing effects" in farmed fish; however, many fish utilize carbohydrates poorly. The intestinal microbiota plays an important role in carbohydrate degradation. Whether the addition of functional bacteria could increase the carbohydrate utilization efficiency and alleviate high-carbohydrate diet-induced adverse effects is unknown.

Results: A bacterial strain that could degrade starch *in vitro* was isolated from the intestines of Nile tilapia (*Oreochromis niloticus*). The bacterium was affiliated to *Bacillus amyloliquefaciens* (designated as *B. amy SS1*) based on 16S rRNA gene sequencing. Three diets, including control diet (CON), high-carbohydrate diet (HCD), and high-carbohydrate diet supplemented with *B. amy SS1* (HCB), were used to feed Nile tilapia for 10 weeks. The beneficial effects of *B. amy SS1* on weight gain and protein accumulation were observed. The HCB decreased blood glucose levels and reduced lipid deposition compared with the HCD group. To detect the possible mechanism, the intestinal microbiota composition was characterized using high-throughput sequencing. The HCB increased the abundance of short-chain fatty acid-producing bacteria. Gas chromatographic analysis indicated that the concentration of acetate increased dramatically in the HCB group compared with that in the HCD group. Glucagon-like peptide-1 (GLP-1) levels increased in the intestine and serum of the HCB group. Different concentrations of sodium acetate (low (HLA), 900 mg/kg; medium (HMA), 1800 mg/kg, and high (HHA), 3600 mg/kg) were added

to the HCD to feed the fish for eight weeks. The HMA and HHA groups mirrored the effects of the HCD supplemented with *B. amy SS1* by increasing serum GLP-1 levels. Increased acetate concentrations stimulated GLP-1 production, which might account for the effects caused by the addition of *B. amy SS1* to the HCD.

Conclusions: This study systematically analyzed the influence of *B. amy SS1* on fish metabolism, suggesting that *B. amy SS1* treatment alleviates the metabolic syndrome caused by HCD by enriching acetate-producing bacteria in fish intestines. Regulating the intestinal microbiota and their metabolites might represent a powerful strategy for fish nutrition modulation and health maintenance in future.

Keywords: Nile tilapia, Intestinal microbiota, SCFA, Metabolism, GLP-1, Carbohydrate utilization

Background

With the increasing cost and limited supply of fishmeal in aquaculture, the utilization of non-protein energy is becoming increasingly important [1]. Carbohydrates are one of the most abundant and cost-effective energy sources [2]. It is commonly accepted that appropriate levels of carbohydrates incorporated into fish diets will decrease the catabolism of protein and lipids to allow for protein sparing effects [3]. However, teleost fish are generally considered to be glucose intolerant [4]. An excess proportion of carbohydrates in their diet causes metabolic syndrome, including decreased growth performance [5], persistent hyperglycemia [6], and excess lipid deposition [7, 8]. The glucose regulation mechanism in fish has been discussed

in numerous studies; however, until now, most metabolic genes related to carbohydrate/glucose utilization have been found to be conserved in vertebrates [9]. These studies suggested that in research on the carbohydrate metabolism characteristics in fish, we need to consider the function of the gut microbiota, which is closely related to host nutrition and metabolism, and is referred as the "second genome" [10].

The intestinal microbiota harbors multiple enzymes for the degradation and fermentation of dietary carbohydrates. Two *Bacteroides* strains, *Bacteroides intestinalis* and *Bacteroides ovatus*, are particularly enriched in genes encoding enzymes for the digestion of carbohydrates [11]. *Ruminococcus bromii* possesses a superior degradative ability with respect to resistant starch, and the released products from resistant starch can be utilized by other gut bacteria to produce short chain fatty acids (SCFAs), which have wide-ranging impacts on host physiology, including serving as an energy source for host cells or stimulating the production of gut hormones [12, 13]. A high-carbohydrate diet altered the fecal microbiome by increasing the carbohydrate degradation members and SCFAs excretion in humans [14]. However, a study in the grass carp (*Ctenopharyngodon idellus*) showed that SCFA levels were lower in the hindgut when they were fed with a high-fiber/low-protein diet compared with that under a high-protein/low-fiber diet [15], indicating that the gut microbiota in the grass carp, which is a predominantly herbivorous fish, does not tend to ferment fiber to SCFAs. These results suggested that the limited utilization efficiency of carbohydrates by the intestinal microbiota

might account for the glucose intolerance of fish.

The intestinal microbiota shows a great potential for maintaining glucose homeostasis; however, the response to regulation by the intestinal microbiota in the context of glucose homeostasis is strongly linked with the baseline microbiota composition. Research on humans with prediabetes showed that exercise-induced changes in the gut microbiota correlated with improved glucose metabolism and insulin sensitivity [16]. The microbiome of responders exhibited an enhanced capacity to produce SCFAs and catabolize branched-chain amino acids, suggesting that the gut microbiota is a key determinant for the variability of glycemic control [16]. A similar observation was made in a cohort of healthy individuals exposed to barley kernel-based bread (BKB), which suggested that humans harboring a higher *Prevotella*/*Bacteroides* ratio exhibited improved glucose metabolism following 3-day consumption of BKB [17]. Fish harbor a *Proteobacteria*-dominated microbiota, which is different from the dominant microbiota in human or mice [18, 19]. Whether regulation of the intestinal microbiota could increase the carbohydrate utilization efficiency and alleviate the adverse effects caused by high-carbohydrate diets in fish remains unknown.

Nile tilapia (*Oreochromis niloticus*) is an economically important fish species and is an ideal fish model for nutritional and metabolic studies because of its fast growth, high resistance to disease, and available genomic information [20]. In the present study, we isolated a strain that could degrade starch *in vitro* from the intestine of Nile tilapia. 16S rRNA gene sequencing showed that the strain was affiliated to

Bacillus amyloliquefaciens (designated as *B. amy SS1*). Three diet treatments, including control diet (CON), high-carbohydrate diet (HCD), and high-carbohydrate diet supplemented with *B. amy SS1* (HCB) were used to feed Nile tilapia for ten weeks. The host physiology and metabolic characteristics were identified in these three groups and the possible mechanism by which *B. amy SS1* regulates carbohydrate utilization was investigated.

Results

A strain isolated from the intestine of Nile tilapia improved the growth performance of fish.

To isolate bacteria that could degrade starch in fish gut, starch was used as the main carbon source in the culture medium. About two hundred colonies were screened and one colony, which had a larger transparent zone on starch agar medium after the addition of iodine solution, was selected for the further research. 16S rRNA gene sequencing showed that the strain was affiliated to *Bacillus amyloliquefaciens* ATCC 39320 (Fig. 1a). The selected strain was named as *B. amy SS1* in the present study. DNS analysis confirmed the amylase activity of *B. amy SS1 in vitro* (Fig. 1b) and gas chromatography showed that *B. amy SS1* could ferment corn starch to mainly produce acetate and butyrate (Fig. 1c).

To detect whether the addition of *B. amy SS1* could influence the growth performance of fish under an HCD, three treatments, including CON, HCD, and HCD with *B. amy SS1* (HCB) were used to feed fish for 10 weeks. Weight gain was

detected every two weeks. The results showed that the average weight was significantly higher in the HCD group than in the CON group; moreover, the average weight was further increased by *B. amy SS1* treatment in the HCB group (Fig. 1d). The addition of *B. amy SS1* to the HCD resulted in the highest weight gain among the three groups (Fig. 1e) and the feed efficiency was higher in the HCB group compared with that in the HCD group (Fig. 1f).

The addition of *B. amy SS1* to the HCD decreased glucose levels by activating the PI3K/AKT insulin signaling pathway and enhancing glycolysis of Nile tilapia.

One of the metabolic disorders caused by HCD is the persistent hyperglycemia in fish [6, 21]. To address whether the addition of *B. amy SS1* to the HCD had a metabolic protective effect, the fasting glucose levels were detected. The results showed that the addition of *B. amy SS1* reduced the high fasting glucose level caused by the HCD (Fig. 2a). The IGTT test showed that the addition of *B. amy SS1* markedly reduced the persistently higher blood glucose level caused by the HCD (Fig. 2b, c), i.e., *B. amy SS1* improved glucose tolerance. Considering the important role of insulin in glucose homeostasis, the fasting insulin level was detected; however, no significant difference was found among the groups (Fig. 2d), suggesting that the addition of *B. amy SS1* to the HCD might elevate insulin sensitivity rather than its amount. Glucose homeostasis induced by *B. amy SS1* was further supported by significantly decreased liver glycogen levels (Fig. 2e). To investigate whether the insulin signaling pathway was activated by the addition of *B. amy SS1*, the expression

levels of crucial proteins, including phosphatidylinositol 3-kinase (PI3K) and protein kinase B (AKT), were detected using western blotting. The total levels of PI3K and AKT were similar among the groups; however, the levels of phosphorylated PI3K and AKT were significantly increased by *B. amy SS1* administration (Fig. 2f, g), suggesting that the addition of *B. amy SS1* to the HCD improved glucose tolerance via activating the PI3K/AKT insulin signaling pathway.

Enhanced glycolysis might improve glucose homeostasis; therefore, three key enzymes of glycolysis, hexokinase (HK), phosphofructokinase (PFK) and pyruvate kinase (PK) were analyzed. The glycolytic enzyme activities in the liver were all increased in *B. amy SS1*-treated fish (Fig. 2h-j). The mRNA expression of glycolysis targeted genes, including *gck*, *pfk*, *pk*, and *ir* in the liver were downregulated in the HCD group, but upregulated by the addition of *B. amy SS1* (Fig. 2k). These data strongly suggested that the addition of *B. amy SS1* to the HCD enhanced glycolysis by activating the pivotal enzymes related to glycolysis in the liver.

The addition of *B. amy SS1* to the HCD reduced lipid deposition by activating the AMPK/ACC signaling pathway to increase energy expenditure in Nile tilapia.

An HCD causes excess lipid accumulation in fish, which further aggravates the metabolic imbalance [22]. The hepatic somatic index (HSI) was mostly increased in the HCD group compared with that in the CON group, and the HCB group showed a decreased trend in HSI, although no significant difference was detected (Fig. 3a). The hepatic lipid content was significantly increased in the HCD group compared with

177 that in the CON group, but it was decreased by the addition of *B. amy SS1* (Fig. 3b).
178 The addition of *B. amy SS1* to the HCD also exhibited protective effects against
179 HCD-induced liver damage, including lower content of triglyceride (TG),
180 non-esterified fatty acid (NEFA), and total cholesterol (T-CHO) in the liver (Fig. 3c-e).
181 Furthermore, hematoxylin eosin staining (H&E) and oil red O staining also indicated
182 that the addition of *B. amy SS1* to the HCD markedly reduced lipid accumulation (Fig.
183 3f-i). The mRNA levels of genes related to lipid synthesis, including *fas*, *accα*, *dgat2*,
184 and *pparγ*, showed no significant difference in the liver among the groups (Fig. 3j).
185 However, compared with that in the HCD group, the HCB group showed substantial
186 up-regulation of genes targeted to lipolysis, including *atgl*, *cpt1*, *hsl*, and *pparα* in the
187 liver (Fig. 3k). These findings suggested that the addition of *B. amy SS1* to the HCD
188 activated lipolysis to decrease lipid deposition in the liver.

189 To address whether activated lipolysis was associated with energy homeostasis,
190 the levels of key proteins involved in this process were detected using western
191 blotting. The phosphorylation of acetyl CoA carboxylase α (ACC), a rate-limiting
192 enzyme of fatty acid synthesis, was inhibited by the addition of *B. amy SS1* to the
193 HCD (Fig. 3l, m). Moreover, the level of phosphorylated AMP-activated protein
194 kinase (AMPK), a key molecule in the regulation of biological energy metabolism,
195 was markedly increased in *B. amy SS1*-treated fish (Fig. 3l, m). Taken together, these
196 results demonstrated that HCD supplemented with *B. amy SS1* reduced lipid
197 deposition by activating the AMPK/ACC signaling pathway, which was likely to
198 increase energy expenditure.

Besides lipid accumulation in the liver, we also detected the content of total lipid in the body. Notably, a decrease in the total lipid content was observed in the *B. amy SS1*-treated fish (Fig. 3n). Moreover, mesenteric fat index (MFI) was lower in HCB group compared with that in the HCD group (Fig. 3o). *B. amy SS1* administration also reduced the cell size of adipocytes (Fig. 3p, q). Meanwhile, the serum TG, NEFA, T-CHO, and low-density lipoprotein (LDL) levels were reduced by the addition of *B. amy SS1* to the HCD, whereas high-density lipoprotein (HDL) levels increased markedly in the *B. amy SS1*-treated fish (Fig. 3r-v). Taken together, these results further demonstrated that the addition of *B. amy SS1* to the HCD reduced lipid deposition in the fish.

The addition of *B. amy SS1* to the HCD increased protein accumulation by activating the mTOR/S6 signaling pathway in Nile tilapia.

We further assessed the impact of *B. amy SS1* on body protein accumulation. The results showed that the addition of *B. amy SS1* to the HCD increased the carcass index and carcass protein content significantly (Fig. 4a, b). The mRNA expression of *mtor* and *s6*, which are related to protein synthesis, were detected. The results indicated that *mtor* was significantly up-regulated by *B. amy SS1* administration, but no significant difference was observed for *s*6 among the groups (Fig. 4c). Western blotting analysis demonstrated that the levels of phosphorylated mTOR and S6 increased significantly after the addition of *B. amy SS1* to the HCD; however, no significant difference was found in the total levels of these proteins (Fig. 4d, e). Overall, these data implied that

221 the HCD supplemented with *B. amy SS1* induced protein accumulation by activating
222 the mTOR/S6 signaling pathway.
223
224 **The addition of *B. amy SS1* to the HCD altered the intestinal microbial**
225 **community composition of Nile tilapia.**
226 The gut microbiota has critical roles in host nutrition and metabolic processes.
227 High-throughput sequencing was used to investigate the effects of *B. amy SS1* on the
228 intestinal microbiota composition. Decreased Ace, Chao1, Shannon, and Sobs indexes
229 in the HCD group were notably increased by *B. amy SS1* treatment (Table 1),
230 suggesting that supplementation with *B. amy SS1* in the HCD restored the richness
231 and diversity of the intestinal microbial community. To assess the overall composition
232 of the bacterial community in the different groups, we analyzed the microbiota
233 composition at the phylum level. The intestinal microbiota was dominated by
234 *Firmicutes*, *Proteobacteria*, *Bacteroidetes*, *Actinobacteria*, and *Fusobacteria* in Nile
235 tilapia (Fig. 5a). Compared with that in the CON group, the HCD group displayed a
236 significant increase in the abundance of *Firmicutes*, while the addition of *B. amy SS1*
237 to the HCD decreased the proportion of *Firmicutes* (Fig. 5b).
238 OTU-based principal co-ordinates analysis (PCoA) revealed that the HCD
239 changed the intestinal microbiota compared with that of the CON group, while the
240 addition of *B.amy SS1* modulated the microbiota composition, resulting in a
241 composition similar to that of the CON group (Fig. 5c). The abundances of 46 OTUs
242 in the HCD group showed significant differences among groups (Fig. 5d). Among

these OTUs, 12 were increased and 34 were decreased in the HCD group, while these OTUs showed the opposite trend in the HCB group. OTU4496, OTU782 (*Streptococcus*), and OTU4496 (*Lactococcus*) were induced by the HCD, but were markedly reduced by the addition of *B. amy SS1*. Moreover, the HCD decreased the abundances of OTU209 (*Weissella*); OTU6174 (*Romboutsia*); OTU938 (*Faecalibacterium*); OTU6929 and OTU2196 (*Ruminococcus*); OTU3573 (*Blautia*); OTU4850 and OTU4857 (*Prevotellaceae*); OTU5921, OTU4958, and OTU3077 (*Bacteroides*); and OTU6083 (*Bifidobacterium*), while the addition of *B. amy SS1* increased the abundances of these OTUs. We noticed that these bacteria were commonly associated with SCFA production [23, 24]. Collectively, these results indicated that compared with that in the HCD group, the addition of *B. amy SS1* to the HCD restored the abundance of SCFA production bacteria in Nile tilapia.

The addition of *B. amy SS1* to the HCD promoted the secretion of GLP-1 via the p38 MAPK pathway.

The results of the previous section showed that the abundance of SCFA-producing bacteria was restored by *B. amy SS1* treatment; therefore, the concentration of SCFAs in the intestines was determined. The result suggested that the reduced concentration of acetate in the HCD group was dramatically elevated by the addition of *B. amy SS1* (Fig. 5e). The propionate content was below the detection limit and the content of butyrate showed marked intra-group difference (data not shown). The mRNA expression of *ffar2*, which encodes free fatty acid receptor 2 (the receptor of SCFAs in

fish), was notably up-regulated in the liver after the addition of *B.amy SS1* to the HCD (Fig. 5f).

Considering glucagon-like peptide (GLP-1) is the main target of FFAR2, the amounts of GLP-1 in the intestine and serum were detected. The results suggested that intestinal and serum GLP-1 levels increased significantly after the addition of *B. amy SS1* to the HCD (Fig. 5g, h). To determine how the signal is transduced, p38 mitogen-activated protein kinases (p38 MAPK), which regulates the production of GLP-1 [25], was detected. The results showed that the level of phosphorylated p38 MAPK was evidently increased by *B.amy SS1* administration, although no significant difference of total p38 MAPK was observed among groups (Fig. 5i, j). These data demonstrated that the increased production of acetate induced by the addition of *B. amy SS1* to the HCD might account for the increased secretion of GLP-1.

Addition of sodium acetate mimicked the effects of *B. amy SS1* supplementation of the HCD.

To further verify the function of microbial metabolites, different concentrations of sodium acetate (HLA, 900 mg/kg; HMA, 1800 mg/kg and HHA, 3600 mg/kg) were added to the HCD to feed Nile tilapia for eight weeks. The fasting glucose test and IGTT showed that blood glucose levels were obviously reduced in the HMA and HHA groups compared with those in the HCD group (Fig. 6a-c), suggesting that the addition of certain concentrations of sodium acetate to the HCD could improve glucose homeostasis of fish. Additionally, the HSI was noticeably decreased in the

HMA and HHA groups (Fig. 6d). In parallel, liver TG levels were reduced in the HMA and HHA groups (Fig. 6e, f). Accordingly, liver histology via H&E staining showed that the percentage of the lipid area exhibited was reduced substantially in the HMA and HHA groups compared with that in the HCD group (Fig. 6g, h). Importantly, we also found that GLP-1 levels were elevated in the serum from the HMA and HHA groups (Fig. 6i). Western blotting analysis revealed that levels of phosphorylated AKT and AMPK increased significantly in the three sodium acetate supplementation groups, while the level of phosphorylated mTOR was only increased in the HMA and HHA groups (Fig. 6j, k). These data indicated that the addition of sodium acetate to the HCD could elevate the secretion of GLP-1 to improve glucose homeostasis and reduce the lipid deposition caused by the HCD, and that these effects are dose-dependent. In brief, the addition of acetate could mimic the metabolic effects caused by addition of *B. amy SS1* to the HCD.

Discussion

Increasing research in humans and other vertebrates have shown that the intestinal microbiota plays an important role in carbohydrate degradation and fermentation [26, 27]. In aquaculture, how to increase the carbohydrate utilization efficiency and alleviate the metabolic syndrome caused by an HCD is vitally important. In the past, administration of benfotiamine and bile acids showed the potential to increase the carbohydrate utilization efficiency in fish [28, 29]; however, the influence of the intestinal microbiota on host carbohydrate metabolism is unknown. In the present

study, *B.amy SS1* isolated from the intestine of Nile tilapia showed an ability to alleviate metabolic syndrome caused by an HCD by restoration of acetate-producing bacteria in the intestines, suggesting that modulation of the intestinal microbiota has great potential to regulate the host metabolism of fish.

The intestinal microbiota produces key enzymes for carbohydrate degradation and fermentation to produced SCFAs, which are considered to be beneficial to the host [11, 30]. Consistent with previous research [15], we also found that the abundance of bacterial members closely related to SCFA production was decreased under an HCD, suggesting that the HCD diminished the numbers of functional bacteria, which might be related to the metabolic syndrome caused by the HCD in fish. The addition of *B. amy SS1* to the HCD restored the bacteria that are believed to be involved in the degradation of carbohydrates or production of SCFAs. OTU209 is affiliated to *Weisells*, which is commonly expanded in a carbohydrate-rich setting and has the ability to ferment polysaccharides to produce SCFAs [24, 31]. OTU938 is affiliated to *Faecalibacterium*, which is one of the dominant bacteria in the hindgut, with higher levels of SCFAs being observed in *Hermosilla azurea* [32]. An expansion of *Faecalibacterium* and significantly greater SCFA concentrations were found in the colon of pigs fed with a high resistant starch diet [33]. The abundance of OTU6929 and OTU2196, belonging to *Ruminococcus*, were increased by the addition of *B. amy SS1* to the HCD. It has been reported that *Ruminococcus* could ferment resistant starch into SCFAs [12, 34]. OTU4850 and OTU4857 are affiliated to *Prevotellaceae*, which were increased in both humans and rats fed with higher dietary starch and are

related to increased SCFA production [23]. We also found that abundance of OTU6083, belonging to *Bifidobacterium*, was lower in the HCD group but enriched in the HCB group. The abundance of *Bifidobacteria* was increased in the human gut by supplementing the diet with resistant starch from potatoes [12].

The metabolic syndrome induced by an HCD are hyperglycemia and hepatic steatosis in mammals [35]. To determine the mechanism by which *B. amy SS1* alleviated these metabolic disorders in fish, we detected the key signaling pathways related to glucose and lipid metabolism. We found that acetate production increased in the intestines of Nile tilapia after the addition of *B. amy SS1* to the HCD. Increased levels of SCFAs stimulate GLP-1 production via the p38 MAPK signaling pathway [25], and in line with the previous research, our results showed higher level of p38 MAPK and GLP-1 in the HCB group. The important roles of GLP-1 in glucose homeostasis and lipid metabolism have been well documented [36, 37]. In mammals, GLP-1 decreases glucose levels via stimulation of insulin release and inhibition of nutrient absorption in the gastrointestinal tract. Meanwhile in teleost fish, it was reported that GLP-1 increased glucose levels via activation of glycogenolysis and gluconeogenesis in the liver [38]. Our results showed that GLP-1 improved glucose homeostasis by enhancing insulin sensitivity to activate the PI3K/AKT insulin signaling pathway in the HCB group, which is consist with findings in mice [39]. Besides glucose homeostasis, GLP-1 also regulates lipid metabolism. GLP-1 suppresses hepatic lipogenesis via activation of the AMPK pathway in chicken and rats [25, 40]. However, to date, there has been no study on the regulation of lipid

353 metabolism by GLP-1 in fish. The results of the present study showed that GLP-1
354 modulated the reduction of lipid deposition by decreasing fatty acid synthesis and
355 activating the AMPK/ACC signaling pathway in the HCB group. Taken together, our
356 results demonstrated that the addition of *B. amy SS1* to the HCD stimulated the GLP-1
357 signaling pathway, which is responsible for the alleviation of metabolic syndrome in
358 fish, suggesting a conserved function of GLP-1 in glucose homeostasis and lipid
359 metabolism between fish and other vertebrates.

360 It is important for fish to produce more body protein in aquaculture [41, 42].
361 Many attempts have been made to increase body protein levels in fish. It was reported
362 that dietary methionine increased protein synthesis by improving amino acid
363 metabolism in turbot (*Scophthalmus maximus L.*) [43]. In the same fish species,
364 replacement of fish meal by soybean meal reduced protein synthesis via
365 nutrient-sensing [44]. In this study, our results showed that the addition of *B. amy SS1*
366 to the HCD increased the carcass protein proportion in fish. Increased protein
367 synthesis is commonly associated with activation of mTOR [45, 46]. Our results
368 showed that the mTOR/S6 signaling pathway was activated in the HCB group. To our
369 knowledge, this is the first study to show a relationship between the intestinal
370 microbiota and protein accumulation in fish, suggesting that the intestinal microbiota
371 might be a new target for protein synthesis in fish.

372 The benefits of sodium acetate have been reported extensively in animals,
373 including improving growth performance, suppressing intestinal inflammation, and
374 maintaining energy homeostasis [47, 48]. Previously, our laboratory found that the

addition of sodium acetate to an HCD could increase the acetate concentration in the intestine of Nile tilapia [48]. In the present study, the addition of sodium acetate to the HCD mirrored the beneficial metabolic effects of *B. amy SS1* supplementation. The addition of a certain concentration of sodium acetate to the HCD could induce the production of GLP-1 to improve glucose tolerance and decrease lipid deposition. It should be noted that phosphorylated mTOR levels increased in the HMA and HHA groups, but no significant difference in the carcass protein content was found among treatments (data not shown). The possible reasons are that the increased protein accumulation might be induced by other microbial metabolites besides acetate, or the feeding period should be prolonged.

Conclusions

In summary, our study demonstrated that the addition of *B. amy SS1*, a bacterium affiliated to *Bacillus amyloliquefaciens*, in an HCD could promote growth performance, improve glucose tolerance, reduce lipid deposition, and increase protein accumulation in Nile tilapia. The addition of *B. amy SS1* to an HCD rebuilt the microbiota composition, and especially, increased the abundance of acetate-producing bacteria in the intestines of fish. The addition of sodium acetate to the HCD mirrored the beneficial effects of *B. amy SS1* supplementation in ameliorating metabolic syndrome. Collectively, this study enhanced our understanding of methods to alleviate metabolic syndrome caused by an HCD in fish by adding functional bacteria, which might represent a novel strategy to regulate fish metabolism.

Methods

Bacteria isolation

Healthy Nile tilapia were anesthetized using MS-222 for 1 h. After 75% alcohol disinfection, the fresh intestinal content was aseptically collected and placed into a pre-weighed sterile tube. The diluted intestinal content was plated on a starch agar medium containing tryptone (10 g/liter), yeast extract (5 g/liter), starch (5 g/liter), sodium chloride (10 g/liter), and agar (0.75 g/liter) at 28 °C overnight. The plates were dropped with Lugol's iodine solution, and the colony with the largest transparent zone was picked and inoculated into Luria-Bertani (LB) broth medium and cultured at 28 °C overnight. The genomic DNA of the strain was extracted using a bacterial genome DNA extraction kit (Tiangen, Beijing, China, DP302) according to the manufacturer's protocol. 16S rRNA was then amplified using primers 27F (5′-AGAGTTTGATCCTGGCTCAG-3′) and 1492R (5′-GGTTACCTTGTTACGACTT-3′). The PCR reaction was performed using the following program: 94 °C for 5 min; 35 cycles at 94 °C for 30 s, 55 °C for 30 s and 72 °C for 90 s; and 72 °C for 10 min. The 16S rRNA gene was sequenced by Majorbio Bio-Pharm Technology Co., Ltd., (Shanghai, China). The similarity of the 16S rRNA sequence of the isolated bacterium to other reference sequences was identified in GenBank (http://blast.ncbi.nlm.nih.gov/Blast.cgi). A phylogenetic tree was constructed using the neighbor-joining method in MEGA 7.0. The bootstrap confidence values were obtained based on 100 replicates. The 16S rRNA gene sequence was submitted to GenBank (NCBI) with the accession number MT226660.

Detection of amylase activity

The amylase activity of the bacterium was detected as described previously [49]. In brief, a 1.0-mL LB broth culture, as a crude enzyme source, was reacted with 4.0 mL of substrate solution (1% starch solution) at 45 °C for 30 min. The enzyme reaction was interrupted by the addition of 1 mL 3,5-dinitrosalicylic acid (DNS) reagent (Leagene, TC0030). The reaction solution was heated for 5 minutes in boiling water and then cooled in running tap water. After the addition of water to 10 mL, the optical density at 540 nm (OD540) of the solution was determined.

Measurement of SCFAs

SCFA concentrations were determined using gas chromatography (GC). First, 200 μL bacteria solution of was mixed with 0.1 mL of 50 % sulfuric acid and vortexed for 30 s. For intestinal SCFA measurement, 0.1 g of intestinal content was homogenized with 0.2 mL of water for 2 min. Then, 0.4 mL of pre-cooled ether was added to the mixture and vortexed for 30 s. The mixture was centrifuged at 12000 × *g* for 10 min at 4 °C. The ether phase was detected in a gas chromatograph (Shimazu, Japan) under the following conditions: An initial column temperature of 100 °C, held for 2 min, increased at a rate of 5 °C/min to 180 °C, and then held for 2 min; the flow rate was kept at 1 mL/min; the inlet temperature was set to 220 °C; and the sample amount was 1 μL with nitrogen as the carrier gas.

Animal feeding experiment

Experiment 1

Nile tilapia juveniles were obtained from Shanghai Ocean University (Shanghai, China). All fish were acclimated at 28 ± 1 °C and fed with a commercial diet (Chengdu, China) twice per day for two weeks. After acclimation, 225 uniformly sized fish (1.63 ± 0.05 g) were randomly distributed into three groups (three replicates for each group, 25 fish per replicate), including a common diet (CON), a high-carbohydrate diet (HCD), and a high-carbohydrate diet supplemented with *B. amy SS1* (HCB). All fish were fed twice daily (8:30 a.m. and 20:30 p.m.) at a feeding rate of 4% body weight. The formulations of the diets are listed in Additional file 1: Table S1. The total weight of fish in each tank was recorded every two weeks, and the feeding amount was adjusted accordingly.

Experiment 2

Four treatments were set up in the second trial: HCD; HCD with a low dose of sodium acetate (900 mg/kg) (HLA); HCD with a medium dose of sodium acetate (1800 mg/kg) (HMA); and HCD with high dose of sodium acetate (3600 mg/kg) (HHA). Three replicates were set for each treatment and each replicate contained 25 fish. The formulations of the diets are listed in Additional file 1: Table S2.

Sampling collection

At the end of each trial, all fish were fasted for 24 h before being weighted. Nine fish from each group (three per tank) were euthanized using MS-222 at 20 mg/L. The liver, muscle, and visceral adipose tissue were collected for subsequent biochemical and

463 molecular biological assays. Blood was collected from the caudal vein and
464 centrifuged to separate the serum (1750 × *g*, 10 min). The serum was immediately
465 frozen at −80 °C for further analysis. The average weight, weight gain, hepatic
466 somatic index (HSI), mesenteric fat index (MFI), and feed efficiency were calculated
467 according to the following formulae:

468 Average weight (g) = Total body weight / Total tails

469 Weight gain (%) = 100 × (Final fish weight−Initial fish weight) / Initial fish
470 weight

471 Hepatic somatic index (HSI, %) = 100 × (Liver weight / body weight)

472 Mesenteric fat index (MFI, %) = 100 × (Mesenteric fat weight / body weight)

473 Carcass protein (%) = 100 × (Carcass weight / body weight)

474 Feed efficiency (%) = 100 × (Final fish weight−Initial fish weight) / Feed intake

475

476 **Detection of body composition**

477 The chemical compositions of the experimental diets and the body composition of
478 Nile tilapia were determined according to standard methods (AOAC) [50]. Moisture
479 was analyzed by drying the samples at 105 °C until they reached a constant weight.
480 Subsequently, samples were pulverized and stored in a glass desiccator at room
481 temperature (25 °C) to analyze the protein and lipid contents. Total lipid was
482 quantified by the method of Bligh and Dyer using a vacuum drying oven (DZF-6050,
483 Jinghong, Ltd, Shanghai, China). Protein was determined by the Kjeldahl method
484 (N × 6.25) using a Kjeltec™ 8200 instrument (Foss, Hoganas, Sweden).

485

486 **Biochemical analysis**

487 Hexokinase (HK), phosphofructokinase (PFK), and pyruvate kinase (PK); glycogen;
488 triglyceride (TG); non-esterified fatty acid (NEFA); total cholesterol (T-CHO);
489 low-density lipoprotein (LDL); and high-density lipoprotein (HDL) were detected
490 using a biochemical assay kit (Nanjing Jiancheng Bioengineering Institute, China).
491 Glucagon-like peptide-1 (GLP-1) was analyzed by using an enzyme-linked
492 immunosorbent assay (ELISA) kit (Hengyuan biotechnology, China). All operations
493 are carried out according to the manufacturer's instructions.

494

495 **Intra-peritoneal glucose tolerance test (IGTT)**

496 An intra-peritoneal injection glucose tolerance test (IGTT) was performed. After 24 h
497 of fasting, 200 mg/kg dextrose solution was administered via intra-peritoneal injection.
498 The blood glucose levels at time 0 (fasting glucose, taken before glucose injection),
499 0.5, 1.5, and 3 hours after glucose injection were analyzed using a OneTouch
500 glucometer (Bayer, USA). The glucose level was plotted against time and the areas
501 under curve (AUC) were calculated using GraphPad Prism 7.0 (GraphPad Software,
502 Inc., La Jolla, CA, USA). The fasting insulin concentration in serum was analyzed
503 using a fish insulin ELISA kit (Hengyuan biotechnology, China).

504

505 **Hematoxylin and Eosin (H&E) Staining**

506 Liver and adipose tissues were fixed in 4% paraformaldehyde. After gradient ethanol

dehydration, the tissues were embedded in paraffin and sliced into 5-μm sections for H&E staining. The histological features were observed and captured under a light microscope (Nikon, Tokyo, Japan). Quantification and statistical analysis were conducted by using Image J (Oracle, USA).

Oil Red O Staining

Oil red O staining was performed to identify the lipid accumulation in the liver. Liver tissue was embedded in optimum cutting temperature compound (OCT, Sakura, USA) and immediately frozen at −80 °C. Approximately 5–10 μm sections were gently flushed with 60% isopropanol for a few seconds. Frozen liver sections were stained with oil red O and counterstained with hematoxylin to visualize the lipid droplets. The histological features were observed and captured under a light microscope (Nikon). Quantification and statistical analysis was conducted using Image J.

Illumina high-throughput sequencing

Genomic DNA extraction from intestinal contents was performed using an E.Z.N.A.® Soil DNA Kit (OMEGA, USA) according to the manufacturer's instructions. DNA quantity and quality were measured using a NanoDrop 2000 Spectrophotometer (Thermo, USA). The V3–V4 region of the bacteria 16S rRNA gene was amplified by PCR using primers 338F (5′-ACTCCTACGGGAGGCAGCA-3′) and 806R (5′-GGACTACHVGGGTWTCTAAT-3′). Unique eight-base barcodes were added to each primer to distinguish the different PCR products. The PCR reactions were

529 performed in a 20 mL mixture containing 4 mL of 5× Fast Pfu Buffer, 2 mL of 2.5
530 mM dNTPs, 0.8 mL of each primer (5 mM), 0.4 mL of FastPfu Polymerase (TransGen,
531 China), and 10 ng of template DNA. The PCR conditions were as follows: 95 °C for 3
532 min; followed by 95 °C for 30 s, 55 °C for 30 s and 72 °C for 45 s for 29 cycles; and
533 extension at 72 °C for 10 min. Purified PCR products were subjected to Illumina
534 based high-throughput sequencing (carried out by Majorbio Bio-Pharm Technology,
535 Co., Ltd.). The raw pair-end reads were subjected to quality-control procedures using
536 Quantitative Insights Into Microbial Ecology (QIIME, version 1.17). The qualified
537 reads were clustered to generate operational taxonomic units (OTUs) at the 97 %
538 similarity level using UPARSE (version 7.1). Chimeric sequences were identified and
539 removed using UCHIME (version 4.1). Taxonomic richness and diversity estimators
540 were determined using the Mothur software. Principal co-ordinates analysis (PCoA)
541 and heat-map analysis were performed in a MATLAB R2016a environment. Forty-six
542 OTUs were selected for heat-map analysis based on: 1) The abundances of these
543 OTUs were higher than 0.01% in each sample; 2) the abundance of these OTUs were
544 significantly different among groups as assessed using the one-way ANOVA with
545 Tukey's adjustment analysis. The high-throughput sequencing data of intestinal
546 microbiota are available in the NCBI short read archive (SRA)
547 (https://www.ncbi.nlm.nih. gov/sra) with the BioProject accession number
548 PRJNA615286.
549
550 **Quantitative Real-time Reverse Transcription PCR (qRT-PCR)**

The total RNA was isolated from tissues by using the TRIzol Reagent (Magen, China). The total RNA concentration was measured using a NanoDrop 2000C spectrophotometer. RNA with an absorbance ratio OD 260/280 between 1.9 to 2.2 and an OD 260/230 greater than 2.0 was used for subsequent analysis. As the template, 800 ng of total RNA was used to synthesize cDNA using a PrimeScript™ RT Reagent Kit (Takara, Japan) in a S1000TM Thermal Cycler (Bio-Rad, USA). The primers for quantitative real-time polymerase chain reaction (qPCR) analysis were designed at NCBI and the sequences are shown in Additional file 1: Table S3. *β-actin* and *ef1α* were used as the reference genes. The qPCR reaction volume was 25 μL containing 2.0 μL of cDNA template, 12.5 μL of 2 × SYBR qPCR Mixture (Aidlab, China), 2.0 μL of PCR primers (5 μM), and 6.5 μL of nuclease-free water and was performed in a CFX96 Connect Real-Time System (Bio-Rad, USA). The qPCR conditions consisted of one cycle at 95 °C for 30 s, followed by 40 cycles at 95 °C for 5 s and an annealing step at 60 °C for 20 s. Melting curves of the amplified products were generated to ensure the specificity of the assays at the end of each qPCR run. The relative gene expression values were calculated by using the $2^{-\Delta\Delta ct}$ method [51].

Western blotting

Radio immunoprecipitation assay (RIPA) (Beyotime Biotechnology, China) containing 1 mM PMSF (Beyotime Biotechnology) was used to extract proteins from liver tissues. Protein concentrations were measured using a BCA Protein Assay Kit (Beyotime Biotechnology). Forty micrograms of protein were subjected to

SDS-PAGE and the separated proteins were transferred to a nitrocellulose membrane. Proteins on the membrane were reacted with the indicated antibodies. Immunoblots were performed using antibodies against the following proteins: phospho-phosphatidylinositol 3-kinase (PI3K) p85 (Tyr458)/p55 (Tyr199) antibody (CST, #4228), phospho-AKT (Ser473) antibody (CST, #4060), phospho-Acetyl Coenzyme A Carboxylase (Ser79) antibody (Abcam, ab31931), phospho-AMP-activated kinase alpha 1 subunit (AMPKα) (Thr172) antibody (CST, #2531), phospho-mechanistic target of rapamycin (mTOR) (Ser2448) antibody (CST, #2971), phospho-S6 ribosomal protein (Ser235/236) antibody (CST, #4856), phospho- p38 mitogen activated protein kinase (p38 MAPK) (Thr180/Tyr182) antibody (Affinity, AF4001), PI3K p85 antibody (CST, #4292), AKT antibody (CST, #9272), AMPKα antibody (CST, #2532), mTOR (CST, #2972), S6 ribosomal protein antibody (CST, #2217), and p38 MAPK antibody (Affinity, AF6456).

Statistical analysis

Statistical analysis of all data was performed using GraphPad Prism 7.0. The results of biological assays are presented as means ± SEM. Datasets were assessed using one-way analysis of variance (ANOVA) with Tukey's adjustment. In the figures: *, $P < 0.05$; **, $P < 0.01$; ***, $P < 0.001$; ****, $P < 0.0001$.

Additional file

Additional file 1. Supplementary Tables S1-S3.

595

596 **Abbreviations**

597 HSI: Hepatic somatic index; MFI: Mesenteric fat index; IGTT: Intra-peritoneal
598 injection glucose tolerance test; OTU: Operational taxonomic unit; PCoA: Principal
599 coordinate analysis; Glucagon-like peptide-1 (GLP-1); Short chain fatty acids
600 (SCFAs); HK: Hexokinase; PFK: Phosphofructokinase; PK: Pyruvate kinase; TG:
601 triglyceride; NEFA: non-esterified fatty acid; T-CHO: total cholesterol; H&E:
602 Hematoxylin eosin staining; ACC: acetyl CoA carboxylase α; AMPK: AMP-activated
603 protein kinase; LDL: low density lipoprotein; HDL: high-density lipoprotein; p38
604 MAPK: p38 mitogen-activated protein kinases; ELISA: enzyme-linked
605 immunosorbent assay.

606

607 # Declarations

608 **Ethics approval and consent to participate**

609 All experiments were conducted under the Guidance of the Care and Use of
610 Laboratory Animals in China. This study was approved by the Committee on the
611 Ethics of Animal Experiments of East China Normal University (F20190101).

612 **Consent for publication**

613 Not applicable.

614 **Availability of data and material**

615 The datasets supporting the conclusions of this article are available in the GenBank
616 repository, [MT226660 (http://blast.ncbi.nlm.nih.gov/Blast.cgi) (16S rRNA)] and in

617 the NCBI short read archive (SRA) [Bioproject PRJNA615286;
618 (https://www.ncbi.nlm.nih. gov/sra) (high-throughput sequencing data of intestinal
619 microbiota)].

620 **Competing Interests**

621 The authors declare that they have no competing interests.

622 **Funding**

623 This work was supported by the National Key R&D program (grant number
624 2018YFD0900400), and the National Natural Science Foundation of China (grant
625 number 31972798).

626 **Authors' contributions**

627 All authors contributed experimental assistance and intellectual input to this study.
628 The original concept was conceived by MLZ and ZYD. Experimental strategies and
629 sampling design were developed by MLZ, ZYD, and LQC. RX and ML performed
630 the feeding experiments. TW and CJS contributed to the collection of samples. RX
631 and YWZ performed the molecular and biochemistry detection. RX performed the
632 bioinformatic analysis of the intestinal samples for microbial composition, and
633 performed the statistical analyses. MLZ, ZYD and FQ contributed to the
634 interpretation of the data. The manuscript was written by MLZ and RX. All authors
635 read and approved the final manuscript.

636 **Acknowledgments**

637 Not applicable.

638 **Author's information**

All of the authors are in School of Life Sciences, East China Normal University, Shanghai, China.

References

[1] Hardy RW. Utilization of plant proteins in fish diets: effects of global demand and supplies of fishmeal. Aquaculture Research 2010;41:770-6.

[2] Maas RM, Verdegem MCJ, Wiegertjes GF, Schrama JW. Carbohydrate utilisation by tilapia: a meta-analytical approach. Reviews in Aquaculture n/a.

[3] Krogdahl Å, Hemre GI, Mommsen TP. Carbohydrates in fish nutrition: digestion and absorption in postlarval stages. Aquaculture Nutrition 2005;11:103-22.

[4] Kamalam BS, Medale F, Panserat S. Utilisation of dietary carbohydrates in farmed fishes: New insights on influencing factors, biological limitations and future strategies. Aquaculture 2017;467:3-27.

[5] Li JN, Xu QY, Wang CA, Wang LS, Zhao ZG, Luo L. Effects of dietary glucose and starch levels on the growth, haematological indices and hepatic hexokinase and glucokinase mRNA expression of juvenile mirror carp (Cyprinus carpio). Aquaculture Nutrition 2016;22:550-8.

[6] Kostyniuk DJ, Marandel L, Jubouri M, Dias K, Souza RFd, Zhang D, et al. Profiling the rainbow trout hepatic miRNAome under diet-induced hyperglycemia. Physiological Genomics 2019;51:411-31.

[7] Prisingkorn W, Prathomya P, Jakovlić I, Liu H, Zhao YH, Wang WM. Transcriptomics, metabolomics and histology indicate that high-carbohydrate diet negatively affects the liver health of blunt snout bream (Megalobrama amblycephala). BMC Genomics 2017;18.

[8] Viegas I, Jarak I, Rito J, Carvalho RA, Metón I, Pardal MA, et al. Effects of dietary carbohydrate on hepatic de novo lipogenesis in European seabass (Dicentrarchus labrax L.). Journal of Lipid Research

661 2016;57:1264-72.

662 [9] Zhang Y, Qin C, Yang L, Lu R, Zhao X, Nie G. A comparative genomics study of
663 carbohydrate/glucose metabolic genes: from fish to mammals. BMC genomics 2018;19:246-.

664 [10] Jia W, Li H, Zhao L, Nicholson JK. Gut microbiota: a potential new territory for drug targeting.
665 Nature Reviews Drug Discovery 2008;7:123-9.

666 [11] Zhang M, Chekan JR, Dodd D, Hong P-Y, Radlinski L, Revindran V, et al. Xylan utilization in
667 human gut commensal bacteria is orchestrated by unique modular organization of
668 polysaccharide-degrading enzymes. Proceedings of the National Academy of Sciences of the United
669 States of America 2014;111:E3708-E17.

670 [12] Baxter NT, Schmidt AW, Venkataraman A, Kim KS, Waldron C, Schmidt TM. Dynamics of human
671 gut microbiota and short-chain fatty acids in response to dietary interventions with three fermentable
672 fibers. mBio 2019;10.

673 [13] Ze X, Duncan SH, Louis P, Flint HJ. Ruminococcus bromii is a keystone species for the
674 degradation of resistant starch in the human colon. The ISME journal 2012;6:1535-43.

675 [14] Fava F, Gitau R, Griffin BA, Gibson GR, Tuohy KM, Lovegrove JA. The type and quantity of
676 dietary fat and carbohydrate alter faecal microbiome and short-chain fatty acid excretion in a metabolic
677 syndrome 'at-risk' population. International Journal of Obesity 2013;37:216-23.

678 [15] Hao YT, Wu SG, Jakovlić I, Zou H, Li WX, Wang GT. Impacts of diet on hindgut microbiota and
679 short-chain fatty acids in grass carp (Ctenopharyngodon idellus). Aquaculture Research
680 2017;48:5595-605.

681 [16] Liu Y, Wang Y, Ni Y, Cheung CKY, Lam KSL, Wang Y, et al. Gut Microbiome Fermentation
682 Determines the Efficacy of Exercise for Diabetes Prevention. Cell Metabolism 2020;31:77-91.e5.

683 [17] Kovatcheva-Datchary P, Nilsson A, Akrami R, Lee Ying S, De Vadder F, Arora T, et al. Dietary
684 Fiber-Induced Improvement in Glucose Metabolism Is Associated with Increased Abundance of
685 Prevotella. Cell Metabolism 2015;22:971-82.
686 [18] Wang AR, Ran C, Ringø E, Zhou ZG. Progress in fish gastrointestinal microbiota research.
687 Reviews in Aquaculture 2018;10:626-40.
688 [19] Bäckhed F, Ley RE, Sonnenburg JL, Peterson DA, Gordon JI. Host-Bacterial Mutualism in the
689 Human Intestine. Science 2005;307:1915.
690 [20] de Verdal H, Vandeputte M, Mekkawy W, Chatain B, Benzie JAH. Quantifying the genetic
691 parameters of feed efficiency in juvenile Nile tilapia Oreochromis niloticus. BMC Genet 2018;19:105-.
692 [21] Conde-Sieira M, Salas-Leiton E, Duarte MM, Pelusio NF, Soengas JL, Valente LMP. Short- and
693 long-term metabolic responses to diets with different protein:carbohydrate ratios in Senegalese sole
694 (Solea senegalensis, Kaup 1858). British Journal of Nutrition 2016;115:1896-910.
695 [22] Xie D, Yang L, Yu R, Chen F, Lu R, Qin C, et al. Effects of dietary carbohydrate and lipid levels
696 on growth and hepatic lipid deposition of juvenile tilapia, Oreochromis niloticus. Aquaculture
697 2017;479:696-703.
698 [23] Cherbuy C, Bellet D, Robert V, Mayeur C, Schwiertz A, Langella P. Modulation of the caecal gut
699 microbiota of mice by dietary supplement containing resistant starch: Impact is donor-dependent.
700 Frontiers in Microbiology 2019;10.
701 [24] Sturino JM. Literature-based safety assessment of an agriculture- and animal-associated
702 microorganism: Weissella confusa. Regulatory Toxicology and Pharmacology 2018;95:142-52.
703 [25] Zhang J-M, Sun Y-S, Zhao L-Q, Chen T-T, Fan M-N, Jiao H-C, et al. SCFAs-Induced GLP-1
704 Secretion Links the Regulation of Gut Microbiome on Hepatic Lipogenesis in Chickens. Frontiers in

Microbiology 2019;10.

[26] He C, Wu Q, Hayashi N, Nakano F, Nakatsukasa E, Tsuduki T. Carbohydrate-restricted diet alters the gut microbiota, promotes senescence and shortens the life span in senescence-accelerated prone mice. Journal of Nutritional Biochemistry 2020;78.

[27] Spring S, Premathilake H, DeSilva U, Shili C, Carter S, Pezeshki A. Low Protein-High Carbohydrate Diets Alter Energy Balance, Gut Microbiota Composition and Blood Metabolomics Profile in Young Pigs. Scientific Reports 2020;10.

[28] Xu C, Liu WB, Dai YJ, Jiang GZ, Wang BK, Li XF. Long-term administration of benfotiamine benefits the glucose homeostasis of juvenile blunt snout bream Megalobrama amblycephala fed a high-carbohydrate diet. Aquaculture 2017;470:74-83.

[29] Yu H, Zhang L, Chen P, Liang X, Cao A, Han J, et al. Dietary Bile Acids Enhance Growth, and Alleviate Hepatic Fibrosis Induced by a High Starch Diet via AKT/FOXO1 and cAMP/AMPK/SREBP1 Pathway in Micropterus salmoides. Frontiers in Physiology 2019;10.

[30] Macfarlane S, Macfarlane GT. Regulation of short-chain fatty acid production. Proceedings of the Nutrition Society 2003;62:67-72.

[31] Lynch KM, Lucid A, Arendt EK, Sleator RD, Lucey B, Coffey A. Genomics of Weissella cibaria with an examination of its metabolic traits. Microbiology 2015;161:914-30.

[32] Fidopiastis PM, Bezdek DJ, Horn MH, Kandel JS. Characterizing the resident, fermentative microbial consortium in the hindgut of the temperate-zone herbivorous fish, Hermosilla azurea (Teleostei: Kyphosidae). Marine Biology 2006;148:631-42.

[33] Haenen D, Zhang J, da Silva CS, Bosch G, van der Meer IM, van Arkel J, et al. A diet high in resistant starch modulates microbiota composition, SCFA concentrations, and gene expression in pig

727 intestine1-3. Journal of Nutrition 2013;143:274-83.

728 [34] Venkataraman A, Sieber JR, Schmidt AW, Waldron C, Theis KR, Schmidt TM. Variable responses

729 of human microbiomes to dietary supplementation with resistant starch. Microbiome 2016;4:33-.

730 [35] Agius L. High-carbohydrate diets induce hepatic insulin resistance to protect the liver from

731 substrate overload. Biochemical Pharmacology 2013;85:306-12.

732 [36] Badman MK, Flier JS. The Gut and Energy Balance: Visceral Allies in the Obesity Wars. Science

733 2005;307:1909-14.

734 [37] Murphy KG, Bloom SR. Gut hormones and the regulation of energy homeostasis. Nature

735 2006;444:854-9.

736 [38] Mojsov S. Glucagon-like peptide-1 (GLP-1) and the control of glucose metabolism in mammals

737 and teleost fish. American Zoologist 2000;40:246-58.

738 [39] Wang Y, Dilidaxi D, Wu Y, Sailike J, Sun X, Nabi X-h. Composite probiotics alleviate type 2

739 diabetes by regulating intestinal microbiota and inducing GLP-1 secretion in db/db mice. Biomedicine

740 & Pharmacotherapy 2020;125:109914.

741 [40] Ben-Shlomo S, Zvibel I, Shnell M, Shlomai A, Chepurko E, Halpern Z, et al. Glucagon-like

742 peptide-1 reduces hepatic lipogenesis via activation of AMP-activated protein kinase. Journal of

743 Hepatology 2011;54:1214-23.

744 [41] Stone DAJ. Dietary carbohydrate utilization by fish. Reviews in Fisheries Science

745 2003;11:337-69.

746 [42] Hemre GI, Mommsen TP, Krogdahl Å. Carbohydrates in fish nutrition: Effects on growth, glucose

747 metabolism and hepatic enzymes. Aquaculture Nutrition 2002;8:175-94.

748 [43] Gao Z, Wang X, Tan C, Zhou H, Mai K, He G. Effect of dietary methionine levels on growth

749 performance, amino acid metabolism and intestinal homeostasis in turbot (Scophthalmus maximus L.).
750 Aquaculture 2019;498:335-42.
751 [44] Xu D, He G, Mai K, Zhou H, Xu W, Song F. Postprandial nutrient-sensing and metabolic
752 responses after partial dietary fishmeal replacement by soyabean meal in turbot (Scophthalmus
753 maximus L.). British Journal of Nutrition 2016;115:379-88.
754 [45] Wang Q, He G, Mai K, Xu W, Zhou H, Wang X, et al. Chronic rapamycin treatment on the
755 nutrient utilization and metabolism of juvenile turbot (Psetta maxima). Scientific Reports 2016;6.
756 [46] Han SL, Wang J, Li LY, Lu DL, Chen LQ, Zhang ML, et al. The regulation of rapamycin on
757 nutrient metabolism in Nile tilapia fed with high-energy diet. Aquaculture 2020;520.
758 [47] Zhang H, Ding Q, Wang A, Liu Y, Teame T, Ran C, et al. Effects of dietary sodium acetate on food
759 intake, weight gain, intestinal digestive enzyme activities, energy metabolism and gut microbiota in
760 cultured fish: Zebrafish as a model. Aquaculture 2020;735188.
761 [48] Li M, Hu F-C, Qiao F, Du Z-Y, Zhang M-L. Sodium acetate alleviated high-carbohydrate induced
762 intestinal inflammation by suppressing MAPK and NF-κB signaling pathways in Nile tilapia
763 (Oreochromis niloticus). Fish & Shellfish Immunology 2020;98:758-65.
764 [49] Bernfeld P. [17] Amylases, α and β. Methods in Enzymology, Academic Press, 1955, pp. 149-58.
765 [50] Cunniff P. Official methods of analysis of AOAC International. Maryland, USA 1997.
766 [51] Livak KJ, Schmittgen TD. Analysis of Relative Gene Expression Data Using Real-Time
767 Quantitative PCR and the 2−ΔΔCT Method. Methods 2001;25:402-8.
768

769 # Figure legends

770 **Fig. 1** Characteristics of *B. amy SS1* isolated from intestine of Nile tilapia *in vitro* and

771 *in vivo*. **a** Phylogenetic tree of *B. amy SS1*. **b** Amylase activity of *B. amy SS1 in vitro.*
772 **c** SCFA production ability of *B. amy SS1 in vitro*. **d** Average weight. **e** Weight gain. **f**
773 Feed efficiency. Data are expressed as mean ± SEM (n = 3 groups). One-way ANOVA
774 with Tukey's adjustment was used for data analysis.
775 **Fig. 2** *B. amy SS1* improved glucose tolerance of Nile tilapia. **a** Fasting blood glucose
776 concentrations. **b** Intra-peritoneal glucose tolerance test (IGTT), glucose levels at 0 h,
777 0.5 h, 1.5 h, and 3 h. **c** Area under the curves of IGTT, #: CON *vs*. HCD, #$P < 0.05$,
778 ##$P < 0.01$; * HCD *vs*. HCB: *$P < 0.05$. **d** Fasting insulin concentrations. **e** Glycogen
779 content in the liver. **f** Western blotting analysis of the levels of p-PI3K and p-AKT in
780 the liver. **g** Quantitation of the levels of p-PI3K and p-AKT normalized to that of
781 GAPDH. **h-j** Glycolytic enzyme activities of HK (h), PFK (i) and PK (j) in the liver. **k**
782 Relative mRNA expression levels of *gck*, *pk*, *pfk*, and *ir* in the liver. Data are
783 expressed as mean ± SEM (n = 6). One-way ANOVA with Tukey's adjustment was
784 used for data analysis.
785 **Fig. 3** *B. amy SS1* reduced lipid deposition of Nile tilapia. **a** Hepatic somatic index. **b**
786 Hepatic lipid content. **c-e** Content of TG (c), NEFA (d) and T-CHO (e) in the liver. **f-i**
787 Histological analysis of liver (n=3), liver tissue stained with H&E (f) and statistical
788 analysis of lipid area percentage (g), liver tissue stained with oil red O (h) and
789 statistical analysis of lipid area percentage (i), scale bar = 100 μm. **j-k** Relative
790 mRNA expression of genes related to lipid synthesis*: fas*, *accα*, *dgat2* and *pparγ* in
791 the liver (j) and lipolysis: *atgl*, *cpt1*, *hsl*, *fatp* and *pparα* in the liver (k). **l** Western
792 blotting analysis of the levels of p-ACC and p-AMPK in the liver. **m** Quantitation of

793 the levels of p-ACC and p-AMPK normalized to that of GAPDH. **n** Total lipid content
794 in the whole body of Nile tilapia at the end of the feeding trial. **o** Mesenteric fat index.
795 **p-q** Histological analysis of fat tissue (n = 3), fat tissue stained with H&E (p) and
796 relative size of adipocyte (q), scale bar = 100 μm. **r-v** Content of TG (r), NEFA (s),
797 T-CHO (t), LDL (u), and HDL (v) in serum. Data are expressed as mean ± SEM (n =
798 6). One-way ANOVA with Tukey's adjustment was used for data analysis.

799 **Fig. 4** *B. amy SS1* increased protein accumulation of Nile tilapia. **a** Carcass index. **b**
800 Carcass protein content. **c** Relative mRNA expression of *mtor* and *s6* in the liver. **d**
801 Western blotting analysis of the levels of p-mTOR and p-S6 in the liver. **e**
802 Quantitation of the levels of p-mTOR and p-S6 were normalized to that of GAPDH.
803 Data are expressed as mean ± SEM (n = 6). One-way ANOVA with Tukey's
804 adjustment was used for data analysis.

805 **Fig. 5** *B. amy SS1* altered the intestinal microbial community composition and
806 microbial metabolites of Nile tilapia. **a** Percent of community abundance at the
807 phylum level. **b** Histogram of community abundance at the phylum level. **c** Principal
808 co-ordinates analysis (PCoA) of the intestinal bacterial community. **d** Heat-map of the
809 bacterial abundance in the intestine. **e** Acetate content in the intestine. **f** Relative
810 mRNA expression of *ffar2* in the liver. **g-h** Content of GLP-1 in intestine (g) and
811 serum (h). **i** Western blotting analysis of the levels of p-p38 MAPK in the liver. **j**
812 Quantitation of the levels of p-p38 MAPK normalized to that of GAPDH. Data are
813 expressed as mean ± SEM (n = 6). One-way ANOVA with Tukey's adjustment was
814 used for data analysis.

Fig. 6 Sodium acetate mirrored the metabolic benefits of *B. amy SS1*. **a** Fasting blood glucose concentrations. **b** Intra-peritoneal glucose tolerance test (IGTT). **c** Area under the curve (AUC) of IGTT. **d** Serum GLP-1. **e** Hepatic somatic index. **f-g** Histological analysis of the liver (n = 3): Liver tissue stained with H&E (f) and statistical analysis of lipid area percentage (g), scale bar =100 μm. **h-i** Content of TG in the liver (h) and serum (i). **j** Western blotting analysis of the levels of phosphorylated p-AKT, p-AMPK, and p-mTOR in the liver. **k** Quantitation of the levels of p-AKT, p-AMPK, and p-mTOR were normalized to that of GAPDH. Data are expressed as mean ± SEM (n = 6). One-way ANOVA with Tukey's adjustment was used for data analysis.

Table 1 ***B. amy SS1*** **changed the intestinal microbial community abundance and diversity of Nile tilapia.**

Figures

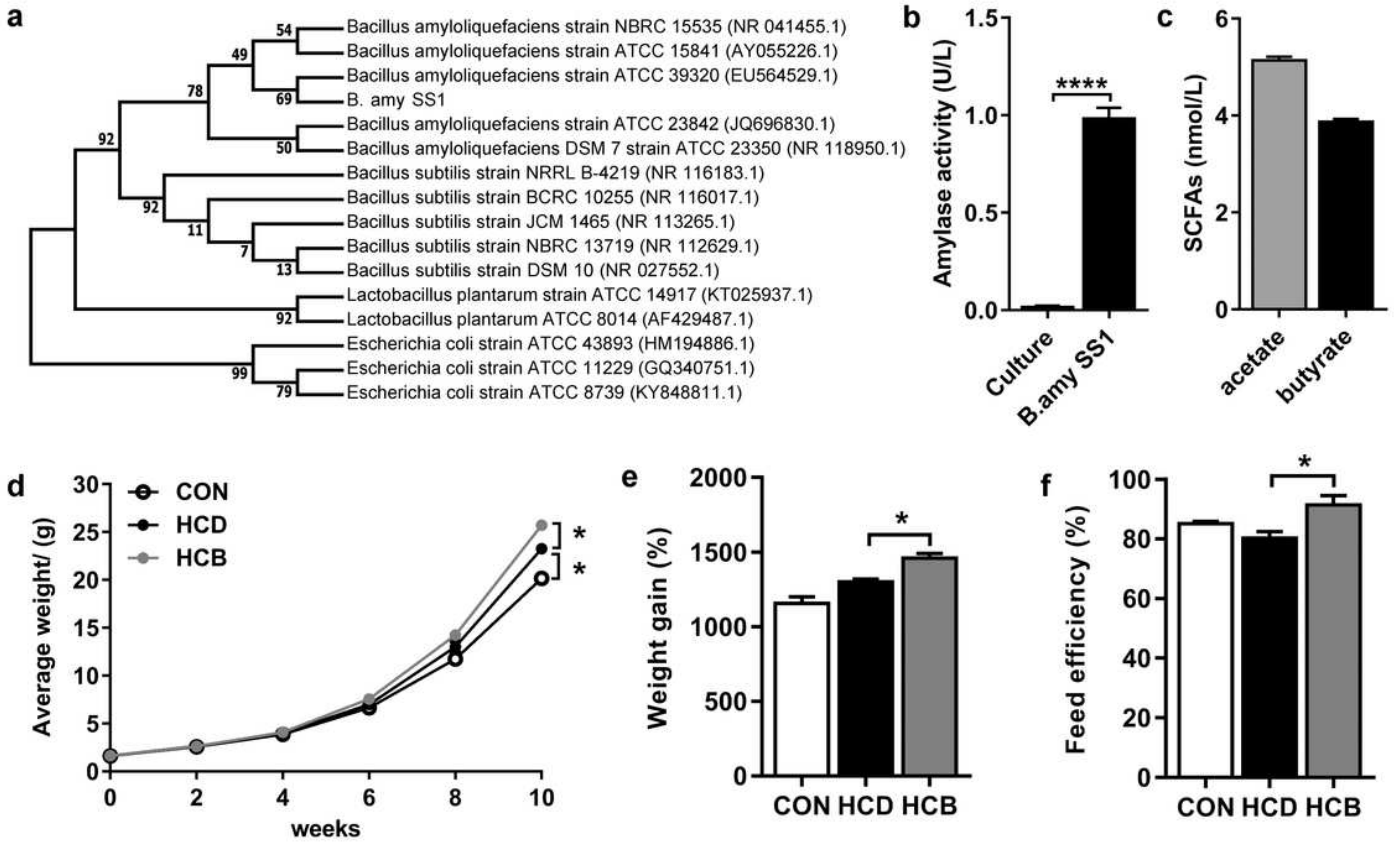

Figure 1

Characteristics of B. amy SS1 isolated from intestine of Nile tilapia in vitro and in vivo. a Phylogenetic tree of B. amy SS1. b Amylase activity of B. amy SS1 in vitro. c SCFA production ability of B. amy SS1 in vitro. d Average weight. e Weight gain. F Feed efficiency. Data are expressed as mean ± SEM (n = 3 groups). One-way ANOVA with Tukey's adjustment was used for data analysis.

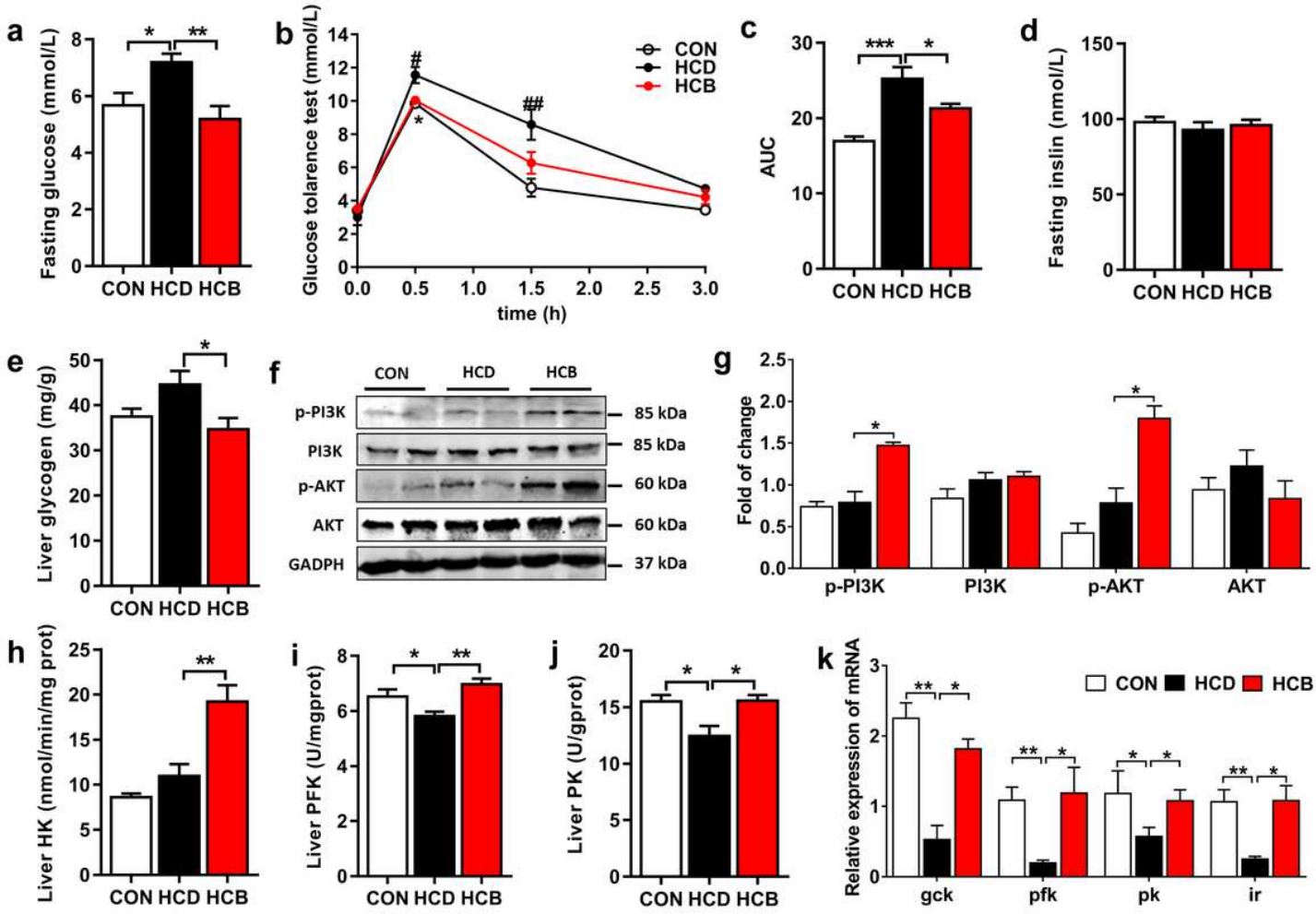

Figure 2

B. amy SS1 improved glucose tolerance of Nile tilapia. a Fasting blood glucose concentrations. b Intra-peritoneal glucose tolerance test (IGTT), glucose levels at 0 h, 0.5 h, 1.5 h, and 3 h. c Area under the curves of IGTT, #: CON vs. HCD, #P < 0.05, ##P < 0.01; * HCD vs. HCB: *P < 0.05. d Fasting insulin concentrations. e Glycogen content in the liver. f Western blotting analysis of the levels of p-PI3K and p-AKT in the liver. g Quantitation of the levels of p-PI3K and p-AKT normalized to that of GAPDH. h-j Glycolytic enzyme activities of HK (h), PFK (i) and PK (j) in the liver. k Relative mRNA expression levels of gck, pk, pfk, and ir in the liver. Data are expressed as mean ± SEM (n = 6). One-way ANOVA with Tukey's adjustment was used for data analysis.

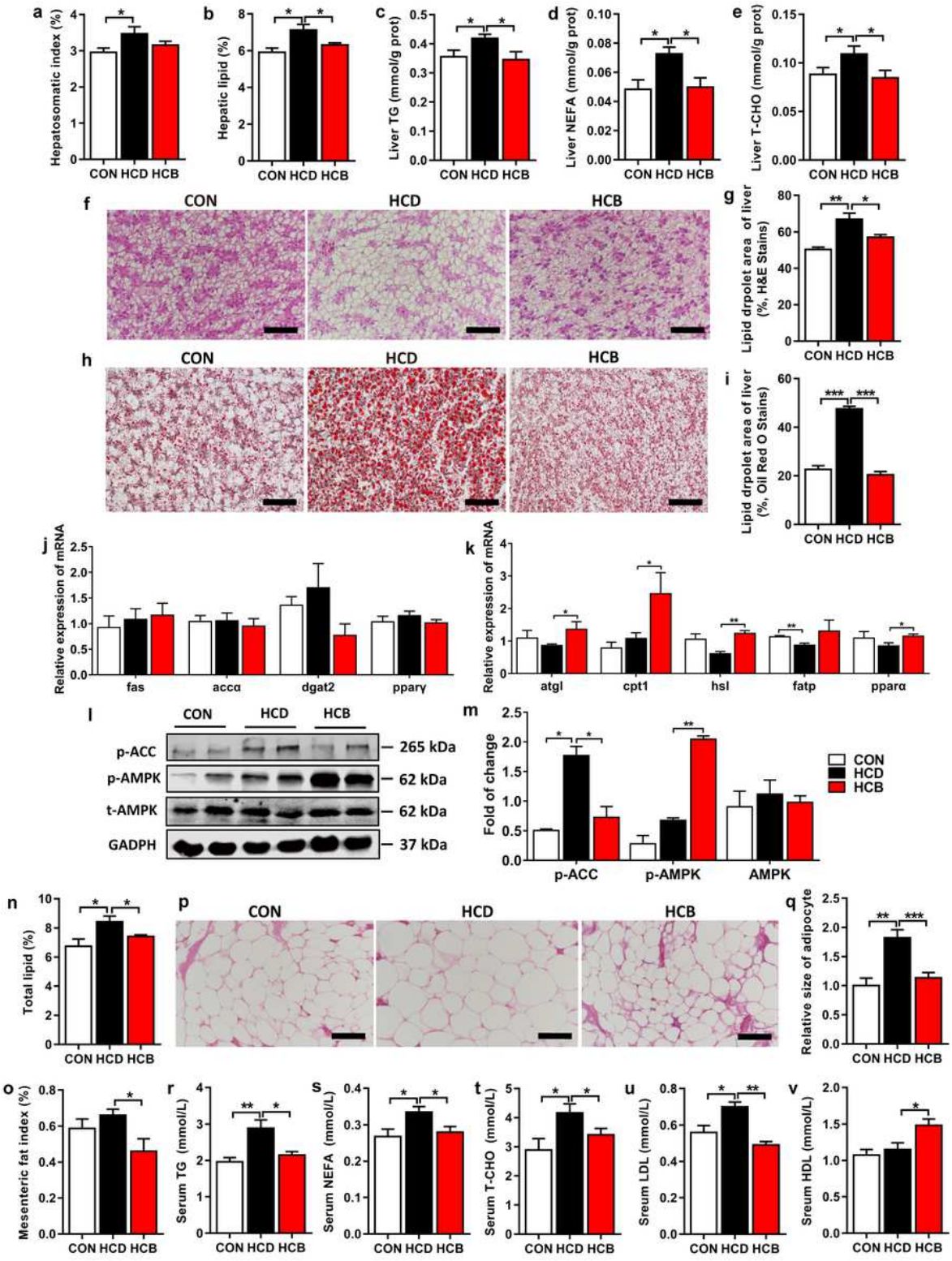

Figure 3

B. amy SS1 reduced lipid deposition of Nile tilapia. a Hepatic somatic index. B Hepatic lipid content. c-e Content of TG (c), NEFA (d) and T-CHO (e) in the liver. f-i Histological analysis of liver (n=3), liver tissue stained with H&E (f) and statistical analysis of lipid area percentage (g), liver tissue stained with oil red O (h) and statistical analysis of lipid area percentage (i), scale bar = 100 μm. j-k Relative mRNA expression of genes related to lipid synthesis: fas, accα, dgat2 and pparγ in the liver (j) and lipolysis: atgl, cpt1, hsl,

fatp and pparα in the liver (k). l Western blotting analysis of the levels of p-ACC and p-AMPK in the liver. m Quantitation of the levels of p-ACC and p-AMPK normalized to that of GAPDH. n Total lipid content in the whole body of Nile tilapia at the end of the feeding trial. o Mesenteric fat index. p-q Histological analysis of fat tissue (n = 3), fat tissue stained with H&E (p) and relative size of adipocyte (q), scale bar = 100 μm. r-v Content of TG (r), NEFA (s), T-CHO (t), LDL (u), and HDL (v) in serum. Data are expressed as mean ± SEM (n = 6). One-way ANOVA with Tukey's adjustment was used for data analysis.

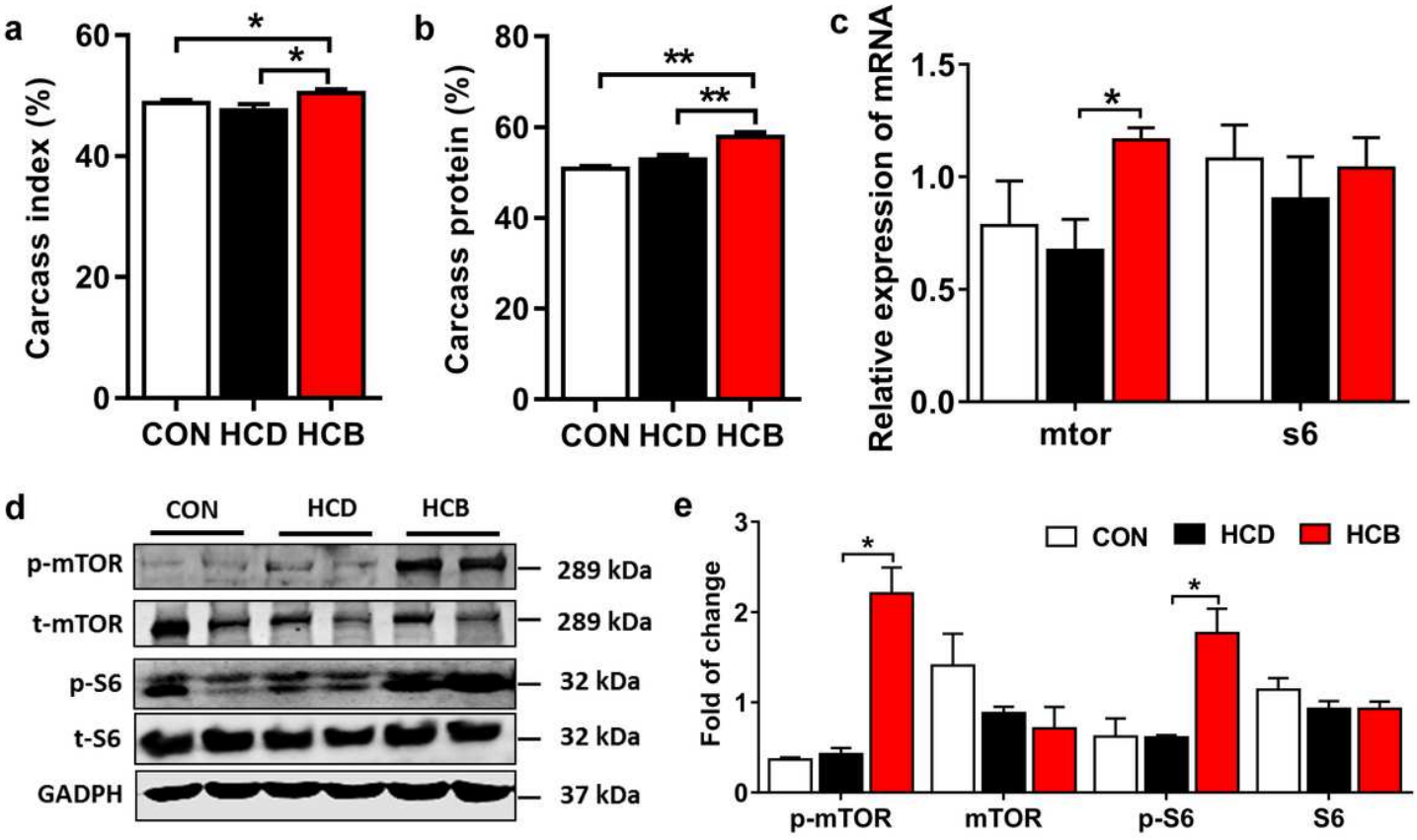

Figure 4

B. amy SS1 increased protein accumulation of Nile tilapia. a Carcass index. B Carcass protein content. c Relative mRNA expression of mtor and s6 in the liver. d Western blotting analysis of the levels of p-mTOR and p-S6 in the liver. e Quantitation of the levels of p-mTOR and p-S6 were normalized to that of GAPDH. Data are expressed as mean ± SEM (n = 6). One-way ANOVA with Tukey's adjustment was used for data analysis.

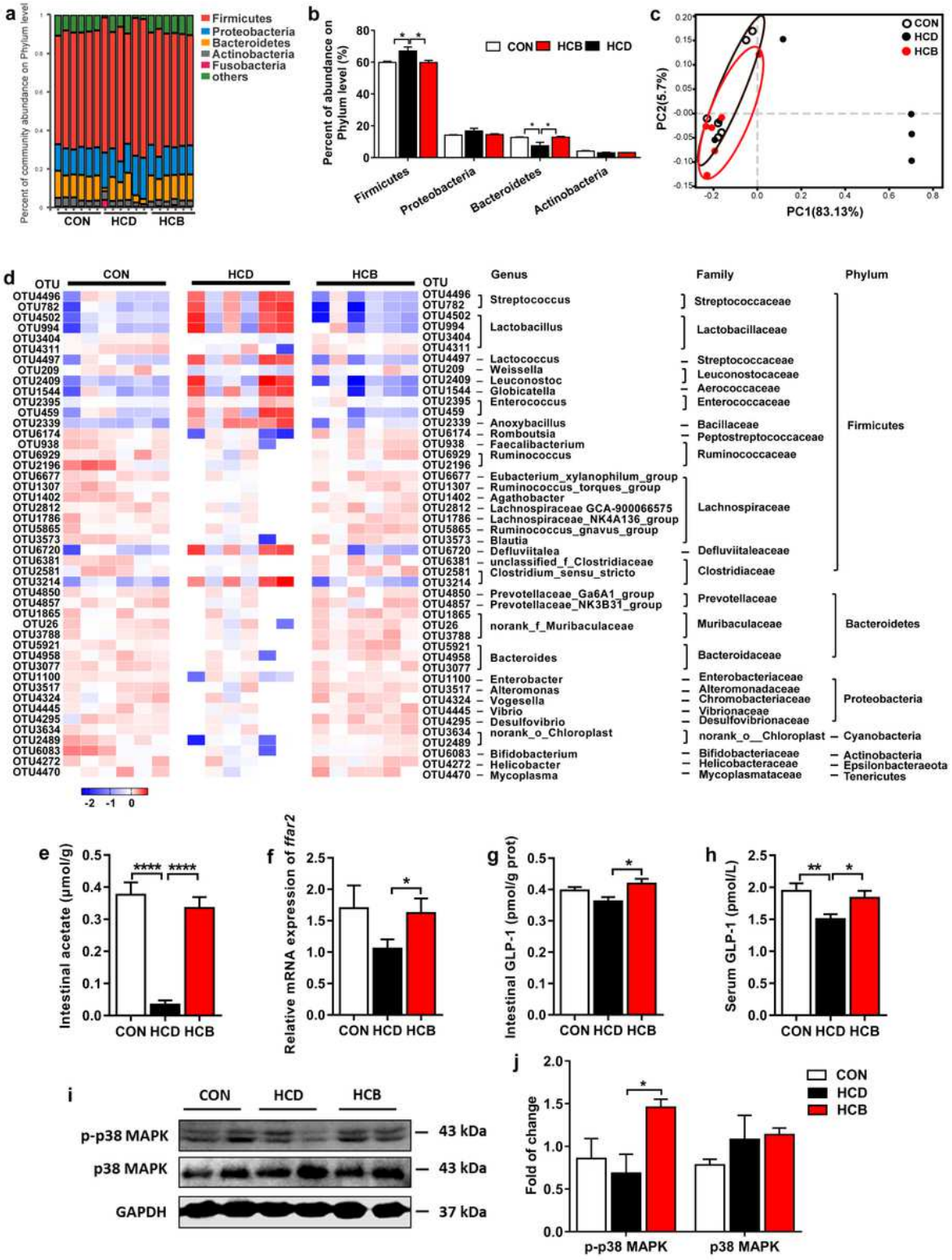

Figure 5

B. amy SS1 altered the intestinal microbial community composition and microbial metabolites of Nile tilapia. a Percent of community abundance at the phylum level. b Histogram of community abundance at the phylum level. c Principal co-ordinates analysis (PCoA) of the intestinal bacterial community. d Heat-map of the bacterial abundance in the intestine. e Acetate content in the intestine. f Relative mRNA expression of ffar2 in the liver. g-h Content of GLP-1 in intestine (g) and serum (h). i Western blotting

analysis of the levels of p-p38 MAPK in the liver. j Quantitation of the levels of p-p38 MAPK normalized to that of GAPDH. Data are expressed as mean ± SEM (n = 6). One-way ANOVA with Tukey's adjustment was used for data analysis.

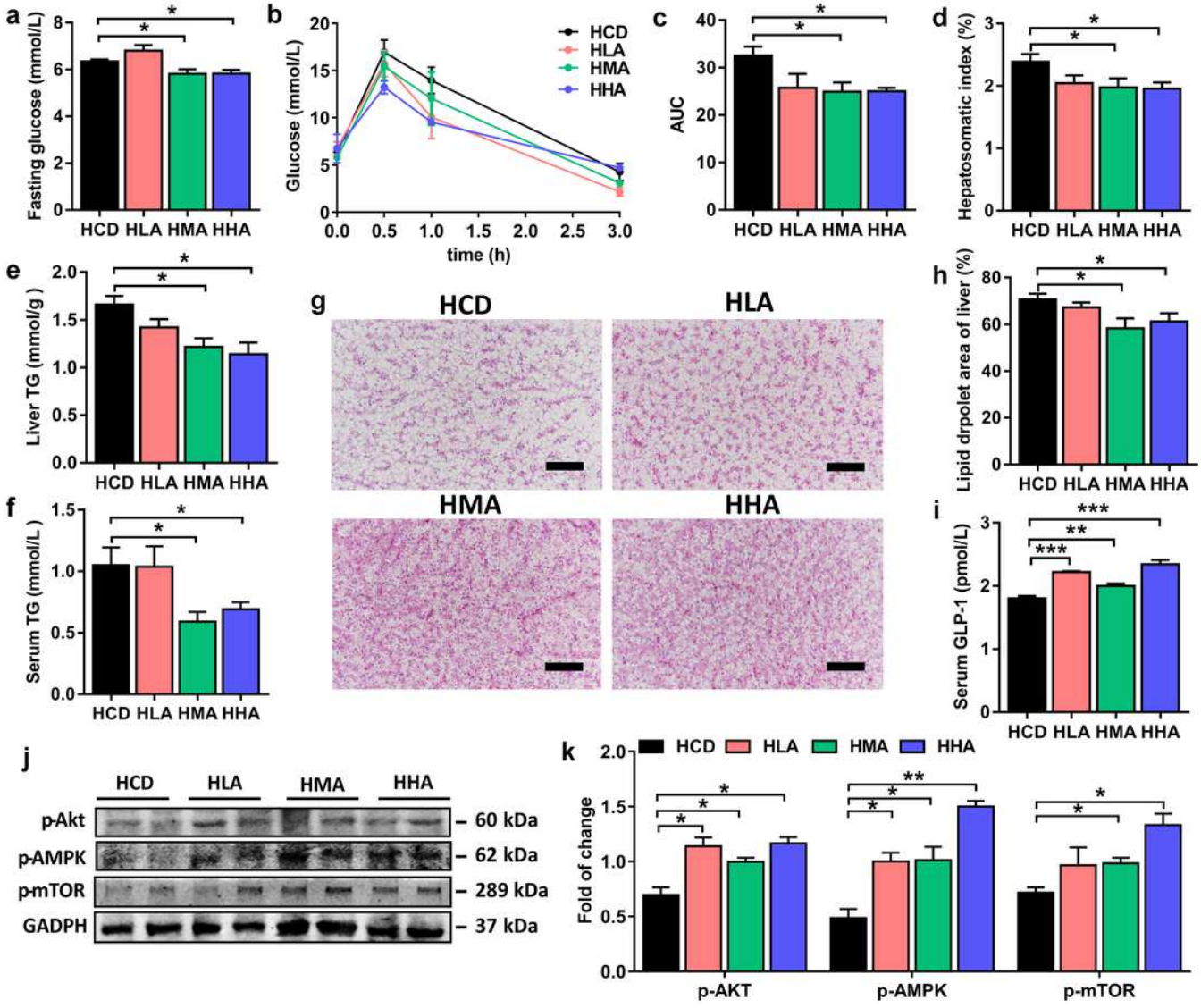

Figure 6

Sodium acetate mirrored the metabolic benefits of B. amy SS1. a Fasting blood glucose concentrations. b Intra-peritoneal glucose tolerance test (IGTT). c Area under the curve (AUC) of IGTT. d Serum GLP-1. e Hepatic somatic index. f-g Histological analysis of the liver (n = 3): Liver tissue stained with H&E (f) and statistical analysis of lipid area percentage (g), scale bar =100 μm. h-i Content of TG in the liver (h) and serum (i). j Western blotting analysis of the levels of phosphorylated p-AKT, p-AMPK, and p-mTOR in the liver. k Quantitation of the levels of p-AKT, p-AMPK, and p-mTOR were normalized to that of GAPDH. Data are expressed as mean ± SEM (n = 6). One-way ANOVA with Tukey's adjustment was used for data analysis.

Supplementary Files

This is a list of supplementary files associated with this preprint. Click to download.

- TableS.docx